Annals of Nuclear Energy 222 (2025) 111550

Contents lists available at ScienceDirect

Annals of Nuclear Energy

journal homepage: www.elsevier.com/locate/anucene

Impact of energy collapsing on the effective neutron lifetime

S. Dulla [a,b,*], N. Abrate [a,b], P. Ravetto [a,b], P. Saracco [b], M. Carta [c,1], V. Fabrizio [c], V. Peluso [d]

[a] Politecnico di Torino, Dipartimento Energia, NEMO Group Corso Duca degli Abruzzi, 24 10129 Torino, Italy
[b] National Institute for Nuclear Physics (I.N.F.N.), Via Dodecaneso, 33 16132 Genova, Italy
[c] ENEA, C.R. Casaccia, Via Anguillarese 301 00123 Roma, Italy
[d] ENEA, C.R. Ezio Clementel, Via Martiri di Monte Sole 4 40129 Bologna, Italy

ARTICLE INFO

Dataset link: https://doi.org/10.5281/zenodo.14454835

Keywords:
Neutron generation time
Multi-group approach
Neutron kinetics
Inverse problems

ABSTRACT

The effective mean prompt neutron generation time (or effective lifetime) is an integral parameter that is introduced in the point kinetic model for nuclear reactor time-dependent analysis. Although such a model requires a strong simplification of the neutron kinetic process, the value of the effective neutron lifetime can give an immediate and useful information on the physical characteristics of a multiplying system and on its time response to perturbations. Furthermore, point kinetics is still used for the simulation of control and transient situations and, especially, in an inverse fashion for the interpretation of neutronic experiments. Based on the standard separation-projection mathematical procedure to derive point kinetics equations, the effective lifetime is defined as the ratio between the total instantaneous importance within the system and the total importance generated by fission per unit time. The evaluation of the effective lifetime can be carried out by both deterministic and stochastic computational tools. Relevant differences can be observed if different physical models are used. In this paper the attention is particularly focused on the energy structure employed. In the first part some analytical analyses for simplified configurations are carried out, in order to gain some physical insight on the effects associated with the detail of the energy group structure on the computed value of the parameter. Then, some more detailed numerical studies allow to investigate more complex configurations. The study includes both critical and subcritical, source-driven systems.

Obituary of Mario Carta (by S. Dulla and V. Fabrizio)

Mario Carta has been a researcher in the field of nuclear reactor physics in ENEA from 1983 to his retirement in 2021. During his long career, he has been involved mainly in the activities on fast neutron reactor physics, supporting the technological deployment of fast reactors, also thanks to the fruitful detachments at CEA-CEN Cadarache (1986–1989) and as a member of the international SPX-1 start-up analysis group. His research work was also focused on the physics of Accelerator Driven Systems, being responsible of different research projects at the national and international level, such as the TRADE physics analysis group under the coordination of C. Rubbia. In 2013 he was appointed Head of the Nuclear Research Reactors Laboratory at C.R. Casaccia, where he coordinated all the activities of the TRIGA and TAPIRO reactors, combining innovation, scientific research and service to society and to external stakeholders. Being in this role, he was also appointed ENEA delegate in different NEA and IAEA working groups and served as Italian delegate in the IAEA Technical Working Group on Research Reactors.

His scientific production shows long, fruitful collaborations with key reactor physics researchers from the 80's and 90's, such as Massimo Salvatores and Pino Palmiotti, combined with the fundamental contribution in raising and helping new generations of experts in reactor physics, in ENEA, in the Italian academia and beyond. After being retired, he kept on dispensing reactor physics wisdom to the young generation of reactor physicists thanks to a collaboration with *new*cleo, and this experience, although tragically cut short by his passing, already impacted largely on the education of his young collaborators actively working on fast reactor technology.

This picture of Mario Carta as an eminent rector physicist of the Italian community is however limited, as it fails to describe the human richness of a man with a multiplicity of passions and skills (music, poetry, literature, grappa tasting,..), hidden right below the surface. As colleagues, we were only able to get a small glimpse at this wonderful universe that Mario was outside of the research work, but we all profited of the direct consequences: his kindness, his sense of humour,

* Corresponding author at: Politecnico di Torino, Dipartimento Energia, NEMO Group Corso Duca degli Abruzzi, 24 10129 Torino, Italy.
E-mail address: sandra.dulla@polito.it (S. Dulla).
[1] Deceased.

https://doi.org/10.1016/j.anucene.2025.111550
Received 6 February 2025; Received in revised form 8 April 2025; Accepted 4 May 2025
Available online 5 June 2025

his capability of being humble without being submissive, his capability to win anyone over with just a joke or a smile.

We consider ourselves lucky as Mario Carta was one of the first person of the reactor physics community we encountered during our education, and he kept his role of teacher, mentor and friend to us from that first day to the last.

The present paper is the outcome of scientific discussions started with Mario at least seven years ago, and some results were already presented at the International Conference PHYSOR 2018 in Cancun, Mexico. That was the last conference we attended together, the occasion for Mario, Massimo Salvatores and Pino Palmiotti to reunite and the luck for all of us to enjoy their company.

1. Introduction

The study of nuclear reactors in transient conditions can be carried out nowadays with detailed simulation tools that are based on some approximations of the time dependent neutron transport equation, such as multi-group diffusion, discrete ordinate or spherical harmonics models (Bell and Glasstone, 1970; Abrate et al., 2020, 2021). It is thus possible to obtain a fairly detailed information of the evolution of the neutron distribution in phase space as a consequence of perturbations introduced into the system by external actions, accidental events and non-linear feedback phenomena. However, this direct approach may be computationally very intensive and it may turn out to be unpractical for some cases, when only some integral information is needed. Consequently, the point kinetics model is still playing an important role in many reactor physics applications, such as the analysis of fast reactors. Its simplicity makes it a viable tool for all inverse evaluations in which some integral parameter is to be retrieved from measurements performed during kinetic experiments. In particular, the point kinetics model is adopted as the basis for the reconstruction and monitoring of the reactivity in subcritical source-driven systems.

The point kinetics model can be derived using the classic Henry's procedure (Henry, 1958), based on a factorization of the solution of the neutron balance equation into the product of a time dependent amplitude function and a time constant shape function, followed by a projection on a suitable weight. The procedure leads to a system of differential equations in the time domain, once delayed emissions are included into the model. These equations contain important integral parameters that physically characterize the system, namely the reactivity, the effective mean prompt neutron generation time, or effective neutron lifetime Λ, the effective delayed neutron fractions and the effective source. It must be noted that one refers to "effective" quantities whenever a weighting is performed on some suitable function, thus taking into account the importance of neutrons in contributing to some specific phenomenon of interest for the observer. Beside the importance of the integral parameters for practical kinetic evaluations, they are also useful to yield an immediate information on the physical properties of the system. This work is focused on the study of the effective neutron lifetime Λ, which is a crucial parameter as it determines the time scale of the neutron response to perturbations or neutron injections.

The direct and absolute measurements of the effective lifetime may be rather difficult. Its estimation by means of computational tools, either deterministic or statistic, is also very challenging. The definition of the parameter itself requires a choice of the weighting function, which may not be fully established and, in any event, is not unique in the case of subcritical systems. In previous works (Dulla et al., 2006; Saracco et al., 2012) the influence of the weight adopted for the definition of kinetic parameters on the accuracy of the results of time-dependent simulations in point kinetics and quasi-statics, with special regards to the case of subcritical systems, was addressed. In the following, it is shown that Λ strongly depends on the neutronic model adopted, in particular on the grid assumed to discretize the energy variable. Such feature was observed and pointed out in the past (Kiefhaber, 1969); in the present work the effect is studied at first analytically for some simple paradigmatic configurations, in order to be able to physically interpret the results. Further analyses are then carried out on a very detailed energy grid and on various coarser energy structures. Relevant differences are evidenced when the adopted number of energy groups becomes very low. Another important effect associated with the averaging procedure for the neutron velocity is analysed in the paper, as this step is performed with different approaches in widely adopted codes for nuclear data collapsing, such as Serpent (Leppänen et al., 2015) and ERANOS (Rimpault et al., 2002). The consequence on the value of the lifetime in the collapsed model may be dramatic, and it has been observed in a past work (Dulla et al., 2015), where extremely large differences were evidenced in the lifetime values when collapsing a 49-group set into a 4-group one with Serpent.

The results of some simulations for subcritical systems (including a system representative of the KUCA reactor (Pyeon et al., 2007) main characteristics) are also presented and discussed. In the final part of the work an analysis of the effect of the value of Λ on relevant neutronic characteristics of the system (e.g. time eigenvalues and stable period) is provided.

2. An analytical exercise

The usual formula for the effective lifetime Λ stems from the factorization/projection procedure proposed by Henry to derive the point reactor kinetic model (Henry, 1958), assuming, as usual, the neutron importance as weighting function. With this approach, the general formula for the neutron effective lifetime reads as:

$$\Lambda = \frac{\langle \phi^\dagger | \hat{V}^{-1} \phi \rangle}{\langle \phi^\dagger | \hat{F} \phi \rangle}, \tag{1}$$

where ϕ is the neutron flux distribution and $\phi^\dagger$ its corresponding adjoint, $\hat{F}$ is the fission emission operator and $\langle \cdot | \cdot \rangle$ the inner product operation, implying integration over the whole phase space. In a multi-group approach the operator $\hat{V}^{-1}$ is represented by a diagonal matrix whose elements are the reciprocal of the group-averaged velocities, $1/\mathrm{v}_g$. While the neutron physical lifetime ℓ represents the average life of the particles in the system, the effective lifetime Λ, also indicated as *"mean neutron prompt generation time"*, takes into account the neutron effectiveness through an adjoint weighting, and therefore it represents the average time spent by the particles to reproduce themselves through fission. As such, the effective lifetime is a physically meaningful parameter for the analysis of multiplying systems. Eq. (1) can be also interpreted as the ratio between the total instantaneous importance in the system (see, e.g. Williams (1991) and Abrate et al. (2023b)) and the importance produced by fission per unit time.

In the following, the analysis is carried out using a multi-group approach: starting from two and three group models, which are considered as reference, the effect of collapsing the original data into a lower number of groups using the standard procedure aimed at preserving reaction rates is investigated. A detailed two-group analysis and some preliminary results were presented at an international conference (Dulla et al., 2018), leading to a shared interest in this topic (Valocchi and Tommasi, 2024).

2.1. From two to one-group for a critical reactor

The two-group model in diffusion theory is considered, first neglecting fast fission (pure thermal reactor) and then including such event. A simple homogeneous system is taken into consideration, assuming both group fluxes distributed according to the fundamental Helmholtz eigenfunction in the critical configuration. The nuclear data (cross sections and inverse velocities) are collapsed into one energy group by averaging on the two-group flux spectrum. The analytical expressions for the reference two-group model and for the resulting one-group model show, as a general result, that the effective lifetime is larger for the two-group evaluations.

Using the definition Eq. (1), the expression for the effective neutron lifetime Λ_{2G} in two-group diffusion with no fast fissions, is written down explicitly as:

$$\begin{aligned}\Lambda_{2G} &= \frac{1}{v_1(D_1B^2+\Sigma_1)} + \frac{1}{v_2(D_2B^2+\Sigma_2)} \\ &= \Lambda_1 + \Lambda_2\end{aligned} \tag{2}$$

The overall effective lifetime thus appears to be the sum of the contributions of the neutrons successively diffusing in the fast and then in the thermal energy ranges, as calculated in the framework of elementary diffusion theory for a homogeneous reactor (Duderstadt and Hamilton, 1976). Although it is not immediately evident from Eq. (2), group 1 acts as a neutron source into group 2, as Σ_1 is the total removal cross section from group 1, and thus includes slowing-down.

Once the equivalent one-group model is constructed, the lifetime takes the form:

$$\begin{aligned}\Lambda_{1G} &= \frac{1}{v_1(D_1B^2+\Sigma_1)} + \frac{1}{v_2(D_2B^2+\Sigma_2)}\frac{\Sigma_{1\to2}}{D_1B^2+\Sigma_1} \\ &= w_{1,2G\to1G}\Lambda_1 + w_{2,2G\to1G}\Lambda_2,\end{aligned} \tag{3}$$

where $w_{g,2G\to1G}$ indicates the weight for the gth group when the data are collapsed from 2 to 1 group. The expressions for these weights are

$$\begin{aligned}w_{1,2G\to1G} &= 1 \\ w_{2,2G\to1G} &= \frac{\Sigma_{1\to2}}{D_1B^2+\Sigma_1}.\end{aligned} \tag{4}$$

A direct comparison of formulae (2) and (3) clearly evidences that the effective lifetime calculated using the equivalent one-group model is shorter. In fact, the weight $w_{2,2G\to1G}$ is always smaller than one, since it is the probability that fast neutrons are slowed down, avoiding fast absorption and leakage. It is also worth observing that the attenuation effect applies to the dominant contribution, since in practical cases $1/v_2$ turns out to be much larger than $1/v_1$. The presence of the q factor appears to introduce a "double counting" of the slowing effect, as such a phenomenon is already fully accounted for in a formula having the structure of Eq. (2), as commented above. A further physical interpretation of the two-group result is related to the proper accounting of a longer collision history: neutrons must first diffuse and suffer collisions to slow down and then conclude their history as thermal neutrons. The one-group model appears to be unable to properly describe such an effect.

A similar result is obtained considering a non-zero fission cross section in both groups, while the emission spectrum is unitary for the first group, consistently with the custom choice of energy boundary for the two-group model. In this case, the analytical expression for the effective lifetime is:

$$\begin{aligned}\Lambda_{2G} &= \frac{1}{v_1(D_1B^2+\Sigma_1)} + \frac{1}{v_2(D_2B^2+\Sigma_2)}\left(1-\frac{\nu\Sigma_{f,1}}{D_1B^2+\Sigma_1}\right) \\ &= w_1\Lambda_1 + w_2\Lambda_2.\end{aligned} \tag{5}$$

After a collapsing process one easily obtains:

$$\begin{aligned}\Lambda_{1G} &= \frac{1}{v_1(D_1B^2+\Sigma_1)} + \frac{1}{v_2(D_2B^2+\Sigma_2)}\left(1-\frac{\nu\Sigma_{f,1}}{D_1B^2+\Sigma_1}\right)\frac{\Sigma_2+D_2B^2}{\nu\Sigma_{f,2}} \\ &= w_{1,2G\to1G}\Lambda_1 + w_{2,2G\to1G}\Lambda_2.\end{aligned} \tag{6}$$

The ratio between the two weighting coefficients for the thermal group reads,

$$\frac{w_{2,2G\to1G}}{w_2} = \frac{\Sigma_2+D_2B^2}{\nu\Sigma_{f,2}}. \tag{7}$$

The value of $w_{2,2G\to1G}$ may be larger or smaller than one, since its value depends on the ratio between the overall removal and the fission production in the lower energy group. In practical applications this ratio is strongly dependent on the energy ranges of each of the two groups. Consequently, the effect can be either a reduction or an increase of the value of Λ in the collapsed model.

2.2. A more involved but instructive example

In an attempt to extend the analysis to a larger number of energy groups and to verify the consistency and the possibility to generalize the results, we consider now a three-group problem, with group boundaries placed at 0.1 and $6.25\cdot10^{-7}$ MeV. Fission neutrons are produced into the fast group, while the intermediate energy group is involved in the moderating process. Due to the cut-off between the thermal and epithermal groups, the up-scattering cross section $\Sigma_{3\to2}$ appears to be non-negligible, especially for fast systems, such as the Lead Fast Reactor and the Molten Salt Fast Reactor, for which a set of representative three-group constants were computed with the Serpent code. Restricting the interest to the fundamental mode only, the following equations are considered:

$$\begin{cases}-(D_1B^2+\Sigma_1)\phi_1 + \frac{1}{k}(\nu\Sigma_{f,1}\phi_1 + \nu\Sigma_{f,2}\phi_2 + \nu\Sigma_{f,3}\phi_3) = 0 \\ \Sigma_{1\to2}\phi_1 - (D_2B^2+\Sigma_2)\phi_2 + \Sigma_{3\to2}\phi_3 = 0 \\ \Sigma_{1\to3}\phi_1 + \Sigma_{2\to3}\phi_2 - (D_3B^2+\Sigma_3)\phi_3 = 0\,.\end{cases} \tag{8}$$

This homogeneous system of algebraic equations has a non-zero solution only if the determinant of its matrix vanishes. The criticality condition can thus be given the following formulation:

$$\begin{aligned}k = &\frac{\nu\Sigma_{f,1}}{D_1B^2+\Sigma_1} + \frac{\nu\Sigma_{f,2}}{D_2B^2+\Sigma_2^*}\left[\frac{\Sigma_{1\to2}}{D_1B^2+\Sigma_1} + \frac{\Sigma_{1\to3}\Sigma_{3\to2}}{(D_1B^2+\Sigma_1)(D_3B^2+\Sigma_3)}\right] \\ &+ \frac{\nu\Sigma_{f,3}}{D_3B^2+\Sigma_3^*}\left[\frac{\Sigma_{1\to3}}{D_1B^2+\Sigma_1} + \frac{\Sigma_{1\to2}\Sigma_{2\to3}}{(D_1B^2+\Sigma_1)(D_2B^2+\Sigma_2)}\right] = 1,\end{aligned} \tag{9}$$

where the terms Σ_2^* and Σ_3^* are defined as follows:

$$\begin{aligned}\Sigma_2^* &= \Sigma_{a,2} + \Sigma_{2\to3}\left(1-\frac{\Sigma_{3\to2}}{D_3B^2+\Sigma_3}\right), \\ \Sigma_3^* &= \Sigma_{a,3} + \Sigma_{3\to2}\left(1-\frac{\Sigma_{2\to3}}{D_2B^2+\Sigma_2}\right).\end{aligned} \tag{10}$$

These modified removal cross sections take into account the fact that neutrons in group 2 (3) may be slowed down (accelerated) to group 3 (2) and come back. In this case, the model yields a correction factor to reduce the overall removal associated with out-group scattering, which is directly proportional to the probability that neutrons come back from a higher or lower energy group. It is possible to generalize the above procedure to any number of energy groups assuming any form of the scattering matrix and of the fission cross section (Saracco et al., 2012).

The explicit form of the flux vector $\vec{\phi}$ and its adjoint $\vec{\phi}^\dagger$ are:

$$\vec{\phi} = \begin{pmatrix} 1 \\ \frac{\Sigma_{1\to2}}{D_2B^2+\Sigma_2} + \frac{\Sigma_{3\to2}}{D_2B^2+\Sigma_2}\left[\frac{\Sigma_{1\to3}}{D_3B^2+\Sigma_3^*} + \frac{\Sigma_{1\to2}\Sigma_{2\to3}}{(D_2B^2+\Sigma_2)(D_3B^2+\Sigma_3^*)}\right] \\ \frac{\Sigma_{1\to3}}{D_3B^2+\Sigma_3^*} + \frac{\Sigma_{1\to2}\Sigma_{2\to3}}{(D_2B^2+\Sigma_2)(D_3B^2+\Sigma_3^*)} \end{pmatrix}, \tag{11}$$

and

$$\vec{\phi}^\dagger = \begin{pmatrix} 1 \\ \frac{\nu\Sigma_{f,2}}{D_2B^2+\Sigma_2} + \frac{\Sigma_{2\to3}}{D_2B^2+\Sigma_2}\left[\frac{\nu\Sigma_{f,3}}{(D_3B^2+\Sigma_3^*)} + \frac{\Sigma_{3\to2}\nu\Sigma_{f,2}}{(D_2B^2+\Sigma_2)(D_3B^2+\Sigma_3^*)}\right] \\ \frac{\nu\Sigma_{f,3}}{D_3B^2+\Sigma_3^*} + \frac{\Sigma_{3\to2}\nu\Sigma_{f,2}}{(D_2B^2+\Sigma_2)(D_3B^2+\Sigma_3^*)} \end{pmatrix}. \tag{12}$$

The neutron lifetime in this scheme can thus be evaluated, obtaining:

$$\begin{aligned}\Lambda_{3G} &= w_1\frac{1}{v_1(D_1B^2+\Sigma_1)} + w_2\frac{1}{v_2(D_2B^2+\Sigma_2^*)} + w_3\frac{1}{v_3(D_3B^2+\Sigma_3^*)} \\ &= w_1\Lambda_1 + w_2\Lambda_2^* + w_3\Lambda_3^*,\end{aligned} \tag{13}$$

Table 1
Group-wise effective lifetimes and weights for LWR, LFR, SFR and MSFR systems using a 3-group model.

	Λ_1 [μs]	Λ_2^* [μs]	w_2 [-]	Λ_3^* [μs]	w_3 [-]	Λ_{3G} [μs]
LWR	0.0184	2.2963	0.901	25.3825	0.750	21.1333
LFR	0.1298	1.0563	0.331	34.7069	0.000	0.4807
SFR	0.1214	1.9039	0.234	16.8198	0.000	0.5748
MSFR	0.0491	1.1363	0.778	27.3468	0.000	0.9439

where Λ_g^* indicates that the neutron lifetime in group g is computed by evaluating the non-leakage probability with Σ_g^*. When $\Sigma_{3\to2} \to 0$, $\Lambda_i^* \to \Lambda_i$. The group-wise weights are $w_1 = 1$,

$$w_2 = \left[\frac{\nu\Sigma_{f,2}}{D_2B^2+\Sigma_2^*}\left(\frac{\Sigma_{1\to2}}{D_1B^2+\Sigma_1}+\frac{\Sigma_{1\to3}\Sigma_{3\to2}}{(D_1B^2+\Sigma_1)(D_3B^2+\Sigma_3)}\right)+ \frac{\nu\Sigma_{f,3}}{D_3B^2+\Sigma_3^*}\frac{\Sigma_{1\to2}\Sigma_{2\to3}}{(D_1B^2+\Sigma_1)(D_2B^2+\Sigma_2)}+ \frac{\Sigma_{1\to3}\nu\Sigma_{f,3}}{D_1B^2+\Sigma_1}\left(\frac{1}{D_3B^2+\Sigma_3^*}-\frac{1}{D_3B^2+\Sigma_3}\right)\right], \tag{14}$$

and

$$w_3 = \left[\frac{\Sigma_{1\to2}\nu\Sigma_{f,2}}{D_1B^2+\Sigma_1}\left(\frac{1}{D_2B^2+\Sigma_2^*}-\frac{1}{D_2B^2+\Sigma_2}\right)+ \frac{\nu\Sigma_{f,2}}{D_2B^2+\Sigma_2^*}\frac{\Sigma_{1\to3}\Sigma_{3\to2}}{(D_1B^2+\Sigma_1)(D_3B^2+\Sigma_3)}+ \frac{\nu\Sigma_{f,3}}{D_3B^2+\Sigma_3^*}\left(\frac{\Sigma_{1\to3}}{D_1B^2+\Sigma_1}+\frac{\Sigma_{1\to2}\Sigma_{2\to3}}{(D_1B^2+\Sigma_1)(D_2B^2+\Sigma_2)}\right)\right], \tag{15}$$

respectively.

Eqs. (13) through (15) help to understand the effects of the various interaction mechanisms on the effective neutron lifetime. First of all, as $\chi_1 = 1$, all newly born neutrons are emitted in the first group. Therefore, each neutron generation lives, on average, at least Λ_1 seconds, and this time is independent of what occurs down-stream in the energy axis. If a neutron survives to leakage and absorption in group 1, it may slow down to epithermal and thermal groups. In these regions, the weight of each group-wise lifetime depends only on the fraction of neutrons spending a certain amount of time in an attempt to induce fission. The fact that only collisions related to the fission process contribute to the *effective* lifetime of the particle is made clear re-writing Eq. (13) without giving the explicit expression for ϕ_2, ϕ_3 and $\phi_2^\dagger$, $\phi_3^\dagger$ at the numerator,

$$\Lambda_{3G} = \frac{\frac{1}{v_1}+\frac{\phi_2}{v_2}\phi_2^\dagger+\frac{\phi_3}{v_3}\phi_3^\dagger}{D_1B^2+\Sigma_1}. \tag{16}$$

In case of vanishing $\Sigma_{2\to3}$ and $\Sigma_{3\to2}$, the importance density for groups 2 and 3 would be directly proportional to $\Sigma_{f,2}$ and $\Sigma_{f,3}$. The limit case of no fission happening in these groups implies that $\phi_2^\dagger = \phi_3^\dagger = 0$, so the slowing down process would not contribute to the effective lifetime.

Table 1 shows the values of the various terms appearing in Eq. (13) obtained considering a homogeneous cylinder with radius R = 65 cm and height H = 152 cm and featured by different sets of realistic homogenized constants, representative of a Light Water Reactor (Ivanov et al., 2013), a Lead Fast Reactor (Grasso et al., 2014), a Sodium Fast Reactor (Fei and Mohamed, 2013) and a Molten Salt Fast Reactor (Abrate et al., 2019, 2023a). The spatially homogenized group constants are reported in Table 2.

Regardless of the way adopted to estimate the group velocity, the weights determining the effective lifetime Λ_{3G} depend only on the group constants. As it can be noticed, w_2 in the LWR and MSFR cases is about 3–4 times larger than the one for the LFR and SFR systems. This difference is mainly caused by $\Sigma_{1\to2}$, which is much larger in LWR and MSFR due to the presence of light elements in the core, e.g. H and Li, respectively.

Despite the values of the lifetime in the low-energy group for the fast systems are even larger than the corresponding ones for the LWR, their associated weights w_3 are negligible, around 10^{-4} and 10^{-5} for the fast reactors: low-energy neutrons could live for a relatively long time in a fast reactor, but this time would have a low value since the probability of inducing fission would be extremely low ($p_{f,3} = \Sigma_{f,3}/\Sigma_{t,3}$ is 0.37% in the SFR, 0.29% in the LFR and 0.32% in the MSFR).

2.3. From three to two-group for a critical reactor

When the three-group constants are collapsed into a two-group structure with a fast and a thermal regions, it is still possible to get an expression for the neutron lifetime that is analogous to Eq. (13),

$$\begin{aligned}\Lambda_{3G\to2G} &= \frac{1}{\bar{k}_{2G}}\frac{1}{\bar{v}_1(\bar{D}_1B^2+\bar{\Sigma}_1^*)}+\frac{1}{\bar{k}_{2G}}\frac{1}{\bar{v}_2(\bar{D}_2B^2+\bar{\Sigma}_2)} \\ &\quad\times\left[\frac{\bar{\Sigma}_{1\to2}}{\bar{D}_1B^2+\bar{\Sigma}_1^*}\left(\frac{\bar{\Sigma}_{2\to1}}{\bar{D}_2B^2+\bar{\Sigma}_2}+\frac{1}{\bar{k}_{2G}}\frac{\bar{\nu}\bar{\Sigma}_{f,2}}{\bar{D}_2B^2+\bar{\Sigma}_2}\right)\right] \\ &= \bar{w}_{1,2G}\frac{1}{\bar{v}_1(\bar{D}_1B^2+\bar{\Sigma}_1^*)}+\bar{w}_{2,2G}\frac{1}{\bar{v}_1(\bar{D}_2B^2+\bar{\Sigma}_2)} \\ &= \bar{w}_{1,2G}\bar{\Lambda}_1^*+\bar{w}_{2,2G}\bar{\Lambda}_2,\end{aligned} \tag{17}$$

where the group constants with the bar symbol are obtained with the collapsing procedure and $\bar{\Lambda}_i$ is obtained using collapsed constants. The collapsed eigenvalue turns out to be

$$\bar{k}_{2G} = \frac{\bar{\nu}\bar{\Sigma}_{f,1}}{\bar{D}_1B^2+\bar{\Sigma}_1^*}+\frac{\bar{\Sigma}_{1\to2}\bar{\nu}\bar{\Sigma}_{f,2}}{(\bar{D}_1B^2+\bar{\Sigma}_1^*)(\bar{D}_2B^2+\bar{\Sigma}_2)}, \tag{18}$$

and may differ from unity if the diffusion coefficient $\bar{D}_1$ is not collapsed by flux-averaging the diffusion coefficients D_1 and D_2.

The physical meaning of $\bar{w}_{2,2G}$ is similar to the one attributed to w_2 and w_3, i.e. the fraction of neutrons that spend their life trying to do fission. It should be noticed that, in practical situations, the cut-off between thermal and fast neutrons is such that $\bar{\Sigma}_{2\to1} \to 0$, so $\Lambda_1^* \to \Lambda_1$. In the case of a thermal reactor, $\bar{\nu}\bar{\Sigma}_{f,1} \to 0$, thus $\bar{w}_{2,2G} \to 1/\bar{k}_{2G}$ and the effective lifetime would simply be the sum of the group lifetimes: each group lifetime is equally *effective* for the fission process, because neutrons are emitted in the fast group but can do fission only in the thermal group.

In order to appreciate the effect of collapsing from three to two energy groups, the weights and the group-wise lifetimes are now expressed as a function of the starting three-group quantities, assuming that $\Sigma_{1\to3} \to 0$, consistently with the discussion made about the data reported Table 2. By making the dependencies with respect to the three-group constants explicit and by manipulating the equations, we can retrieve the following expression,

$$\Lambda_{3G\to2G} = w_{1,2G}\Lambda_1 + w_{2,2G}\Lambda_2^* + w_{3,2G}\Lambda_3^*, \tag{19}$$

where Λ_1, Λ_2^* and Λ_3^* have the same meaning of Eq. (13), $w_{1,2G} = 1$ while $w_{2,2G}$ and $w_{3,2G}$ are defined as

$$w_{2,2G} = \frac{\Sigma_{1\to2}}{D_1B^2+\Sigma_1} \tag{20}$$

and

$$\begin{aligned}w_{3,2G} &= \frac{\Sigma_{1\to2}}{D_1B^1+\Sigma_1}\frac{\Sigma_{2\to3}\left(\Sigma_{3\to2}+\frac{\nu\Sigma_{f,3}}{\bar{k}_{2G}}\right)}{(D_2B^2+\Sigma_2)(D_3B^2+\Sigma_3)} \\ &= w_{2,2G}\frac{\Sigma_{2\to3}\left(\Sigma_{3\to2}+\frac{\nu\Sigma_{f,3}}{\bar{k}_{2G}}\right)}{(D_2B^2+\Sigma_2)(D_3B^2+\Sigma_3)},\end{aligned} \tag{21}$$

respectively. The notation $w_{i,2G}$ indicates the ith weight obtained by collapsing from three to two groups.

The comparison of Eq. (20) with Eq. (14) shows that the weight in the two-group formalism does not depend anymore directly on the number of neutrons emitted by fission, but only on the fraction of

Table 2
Three-group constants used for calculating the parameters in Table 1.

	LWR			LFR			SFR			MSFR		
g	1	2	3	1	2	3	1	2	3	1	2	3
D_g	1.0764	0.4221	0.2524	1.2338	0.80604	0.7048	1.5508	0.8138	0.4519	1.1423	1.1251	0.6213
$\Sigma_{r,g}$	0.0466	0.0521	0.0959	0.0073	0.0053	0.0327	0.0075	0.0058	0.0698	0.0202	0.0074	0.0461
$\Sigma_{f,g}$	0.0017	0.0033	0.0474	0.0022	0.0018	0.0014	0.0023	0.0013	0.0027	0.0015	0.0028	0.0017
$\nu\Sigma_{f,g}$	0.0048	0.0088	0.1223	0.0064	0.0051	0.0038	0.0080	0.0045	0.0098	0.0049	0.0093	0.0056
χ_g	1.0	0.0	0.0	1.0	0.0	0.0	1.0	0.0	0.0	1.0	0.0	0.0
$\Sigma_{g\to1}$	0.2631	0.0	0.0	0.2629	0.0	0.0	0.2074	0.0	0.0	0.2717	0.0	0.0
$\Sigma_{g\to2}$	0.0440	0.7377	0.0016	0.0042	0.4082	0.0128	0.0040	0.4037	0.0229	0.0176	0.2888	0.0187
$\Sigma_{g\to3}$	0.0	0.0341	1.2247	0.0	0.0	0.4402	0.0	0.0	0.6678	0.0	0.0	0.4904

neutrons slowed down from 1 to 2. This new coefficient reflects the fact that, in the two-group model, fast and epithermal neutrons have the same importance[2] but different lifetimes, which thus should be weighted with the slowing down probability. Despite this physical expectations, Eq. (20) seems to lose the effect of neutrons that transit in the epithermal group in order to do fission in the thermal group. The ratio between $w_{2,2G}$ and w_2 has a specific physical meaning,

$$\frac{w_{2,2G}}{w_2} = \frac{1}{\dfrac{\nu\Sigma_{f,2}}{D_2B^2+\Sigma_2^*} + \dfrac{\nu\Sigma_{f,3}}{D_3B^2+\Sigma_3^*}\dfrac{\Sigma_{2\to3}}{D_2B^2+\Sigma_2}} = \frac{\dfrac{\Sigma_{1\to2}}{D_1B^2+\Sigma_1}}{1-\dfrac{\nu\Sigma_{f,1}}{D_1B^2+\Sigma_1}} = \frac{\#\text{ neutrons slowed down}}{\#\text{ neutrons multiplied below fast region}}, \tag{22}$$

which can be useful to understand how the "collapsed" models weight the epithermal lifetime for the various reactor types. For a thermal system the ratio tends to be smaller than one, since $\nu\Sigma_{f,1}\to0$, while for a fast system the value of the ratio can be larger than 1. For the MSFR-like system, the number of neutrons slowing down from group 1 to group 2 is larger (0.794) than the number of neutrons multiplying in groups 2 and 3 (0.778), so the ratio is larger than 1. This situation is verified for the SFR and LFR as well, despite the numerator (0.386 and 0.440, respectively) and denominator (0.234 and 0.332, respectively) are lower.

The ratio between the weights associated with the thermal lifetime is

$$\frac{w_{3,2G}}{w_3} = \frac{\dfrac{\Sigma_{3\to2}}{D_3B^2+\Sigma_3} + \dfrac{1}{\bar{k}_{2G}}\dfrac{\nu\Sigma_{f,3}}{D_3B^2+\Sigma_3}}{\dfrac{\Sigma_{3\to2}\nu\Sigma_{f,2}}{(D_3B^2+\Sigma_3^*)(D_2B^2+\Sigma_2)} + \dfrac{\nu\Sigma_{f,3}}{D_3B^2+\Sigma_3^*}}. \tag{23}$$

The coefficient w_3 provides the fraction of neutrons transiting in group 2 with the aim of doing fission, while $w_{3,2G}$, i.e. the weight computed with the collapsed constants, does not yield the same physical quantity. Assuming that $\Sigma_{3\to2}\to0$, the ratio would tend to $1/\bar{k}_{2G}$. Despite the ratio is larger than 1 for SFR, LFR and MSFR (1.38, 1.33 and 1.02, respectively), it should be remarked that the absolute value of the weight is so small that the collapsing effect for the thermal lifetime is negligible. On the contrary, this effect is more relevant for the LWR case, since the weight is relatively large. In this last case, the ratio is smaller than 1, i.e. the thermal lifetime is underestimated with respect to the three-group case.

The results showed in this section suggest that, for thermal systems like LWRs, the group collapsing process reduces both the epithermal and thermal lifetimes, while for fast systems, like LFR and MSFR, the situation is reversed. While underestimating Λ may be conservative for LWR, its overestimation can seriously impact the reactor dynamic calculation of fast reactors, therefore this effect should be carefully taken into account when few-group calculations are used to estimate the kinetic parameters.

[2] Note that the group constants are collapsed by preserving the reaction rates, not the adjoint-weighted reaction rates.

2.4. From three- to one-group for a critical reactor

In this section, we show the effect of further collapsing the group constants, moving to a one-group model. At first, the two-group constants are collapsed to one-group,

$$\begin{aligned}\Lambda_{2G\to1G} &= \frac{\dfrac{1}{\bar{v}}}{\bar{v}\bar{\Sigma}_f} = \frac{1}{\bar{k}_{2G}}\frac{1}{\bar{v}_1(\bar{D}_1B^2+\bar{\Sigma}_1^*)} + \frac{1}{\bar{k}_{2G}}\frac{1}{\bar{v}_2(\bar{D}_2B^2+\bar{\Sigma}_2)}\frac{\bar{\Sigma}_{1\to2}}{\bar{D}_1B^2+\bar{\Sigma}_1^*} \\ &= \bar{w}_{1,1G}\frac{1}{\bar{v}_1(\bar{D}_1B^2+\bar{\Sigma}_1^*)} + \bar{w}_{2,1G}\frac{1}{\bar{v}_2(\bar{D}_2B^2+\bar{\Sigma}_2)} \\ &= \bar{w}_{1,1G}\bar{\Lambda}_1^* + \bar{w}_{2,1G}\bar{\Lambda}_2\end{aligned} \tag{24}$$

where the $\bar{v}$ and $\bar{v}\bar{\Sigma}_f$ are the one-group velocity and fission production cross section, while the symbols with the bar and the ith subscript refer to the ith group of the two-group model.

The previous expression can be easily compared to Eq. (17). The first term is equal for both cases, while the weight of the thermal lifetime depends on the specific features of the system. For a thermal system $\Sigma_{f,1}\to0$ and $\Sigma_{2\to1}\to0$, so $w_{2,2G}\to1$, while $w_{2,1G}$ would tend to the slowing down probability, yielding a shorter effective lifetime. For fast systems, the term in round parentheses is smaller than 1, meaning that also in this case the thermal lifetime has a larger weight compared to the one estimated with the two-group model.

If the collapsed two-group constants are replaced with their definitions, the lifetime turns out to be

$$\begin{aligned}\Lambda_{3G\to1G} &= \frac{1}{v_1(D_1B^2+\Sigma_1)} + \frac{1}{v_2(D_2B^2+\Sigma_2^*)}\frac{\Sigma_{1\to2}}{D_1B^2+\Sigma_1} + \\ &\quad \frac{1}{v_3(D_3B^2+\Sigma_3^*)}\frac{\Sigma_{1\to2}\Sigma_{2\to3}}{(D_2B^2+\Sigma_2)(D_3B^2+\Sigma_3)} \\ &= w_{1,1G}\frac{1}{v_1(D_1B^2+\Sigma_1)} + w_{2,1G}\frac{1}{v_2(D_2B^2+\Sigma_2^*)} \\ &\quad + w_{3,1G}\frac{1}{v_3(D_3B^2+\Sigma_3^*)}.\end{aligned} \tag{25}$$

This expression allows to have a clearer picture of the effect of the group collapsing. As expected, $w_{2,1G}=w_{2,2G}$, since the fast and epithermal groups are collapsed together in the two- and one-group models. The weight of the thermal group $w_{3,1G}$ appears similar to $w_{3,2G}$, but does not consider neither the up-scattering nor the thermal fission. As discussed above, the collapsing process based on the preservation of the forward reaction rates does not allow to preserve, at the same time, the adjoint reaction rates. Therefore, each collapsing process deteriorates the adjoint vector. The limit case is the one-group model: the absence of any energy effect makes the forward and adjoint vectors coincide. In such a case, the weights of each group lifetime are proportional to the

Table 3
Effective lifetimes obtained after collapsing for LWR, LFR, SFR and MSFR data onto a 2- and 1-group grid.

	Λ_{3G} [μs]	$\Lambda_{3G\to 2G}$ [μs]	$\Lambda_{3G\to 1G}$ [μs]
LWR	21.1333	20.9625	16.9857
LFR	0.4807	0.59574	0.59671
SFR	0.5748	0.86708	0.87884
MSFR	0.9439	0.96211	0.97190

fraction of neutrons slowed down from group 1 to 2 and from group 1 to 3.

The numerical results obtained after collapsing the 3-group constants reported in Table 2 onto the 2- and 1-group grids are reported in Table 3. These results support the observation made previously: the collapsing process tends to reduce the effective lifetime for thermal systems and to increase the one for fast systems.

2.5. Different definitions of the effective lifetime

The effective lifetime given in formula (1) constitutes the standard definition consistent with the classical Henry's derivation of the point kinetic model (Henry, 1958). However, alternative approaches could lead to different definitions, in particular assuming different weights in the projection procedure (Dulla et al., 2006). We present here the limiting peculiar case of assuming a constant weight in the definition of the lifetime:

$$\Lambda = \frac{\left\langle 1 \left| \hat{V}^{-1}\phi \right. \right\rangle}{\left\langle 1 \left| \hat{F}\phi \right. \right\rangle}. \tag{26}$$

It can be easily shown that in such a case the three-group definition becomes

$$\begin{aligned}\Lambda_{3G} = &\frac{1}{\mathrm{v}_1(D_1B^2+\Sigma_1)} + \frac{1}{\mathrm{v}_2(D_2B^2+\Sigma_2^*)}\frac{\Sigma_{1\to 2}}{D_1B^2+\Sigma_1} \\ &+\frac{1}{\mathrm{v}_3(D_3B^2+\Sigma_3^*)}\frac{\Sigma_{1\to 2}\Sigma_{2\to 3}}{(D_2B^2+\Sigma_2)(D_3B^2+\Sigma_3)},\end{aligned} \tag{27}$$

and is unchanged when either dealing with a fast or thermal system. When collapsing to two- and one-group energy structures, the same formula is obtained, and the same happens for the other kinetic parameters, such as the effective delayed neutron fraction β. This is a direct consequence of the fact that these definitions are based on ratios of reaction rates, which are preserved in the energy averaging procedure. Similar results could be found as well also for larger number of energy groups. Despite the preservation of the reaction rates and, thus, of the Λ value, this alternative definition does not clearly account for the importance associated with neutrons, thus yielding quite different results with respect to those obtained in the standard definition, which is instead consistent with the classic derivation of point kinetics.

2.6. Sub-critical systems

In this section, we focus on sub-critical systems, as the case allows different possibilities for the definition of the kinetic parameters.

In the case of no external source, the steady state is guaranteed introducing the effective multiplication eigenvalue k_d, which is lower than 1. The two group diffusion model yields the following direct

$$\begin{cases}\left(D_1B^2+\Sigma_1-\dfrac{\nu\Sigma_{f,1}}{k_d}\right)\phi_1-\dfrac{\nu\Sigma_{f,2}}{k_d}\phi_2=0\\ -\Sigma_{1\to 2}\phi_1+(D_2B^2+\Sigma_2)\phi_2=0\end{cases} \tag{28}$$

and adjoint equations,

$$\begin{cases}\left(D_1B^2+\Sigma_1-\dfrac{\nu\Sigma_{f,1}}{k_d}\right)\phi_1^\dagger-\Sigma_{1\to 2}\phi_2^\dagger=0\\ -\dfrac{\nu\Sigma_{f,2}}{k_d}\phi_1^\dagger+(D_2B^2+\Sigma_2)\phi_2^\dagger=0,\end{cases} \tag{29}$$

whose solutions are

$$\vec{\phi}=\begin{pmatrix}1\\ \dfrac{\Sigma_{1\to 2}}{D_2B^2+\Sigma_2}\end{pmatrix}, \tag{30}$$

and

$$\vec{\phi}^\dagger=\begin{pmatrix}1\\ \dfrac{\nu\Sigma_{f,2}}{k_d(D_2B^2+\Sigma_2)}.\end{pmatrix}, \tag{31}$$

The effective multiplication factor is defined as

$$k_d=\frac{\nu\Sigma_{f,1}}{D_1B^2+\Sigma_1}+\frac{\nu\Sigma_{f,2}\Sigma_{1\to 2}}{(D_1B^2+\Sigma_1)(D_2B^2+\Sigma_2)}. \tag{32}$$

Using the critical solutions, the effective lifetime becomes

$$\Lambda_{2G}=\frac{1}{k_d}\left(\frac{1}{v_1(D_1B^2+\Sigma_1)}+\frac{1}{v_2(D_2B^2+\Sigma_2)}\left(1-\frac{\nu\Sigma_{f,1}}{k_d(D_1B^2+\Sigma_1)}\right)\right), \tag{33}$$

which is the usual interpretation of the effective lifetime as the ratio between the neutron removal lifetime and the effective multiplication parameter of the system.

Collapsing the model into a one-group model with the critical shape expressed in Eq. (30) and Eq. (31), the effective lifetime of the one-group model becomes

$$\begin{aligned}\Lambda_{2G\to 1G}&=\frac{1}{k_d}\left(\frac{1}{v_1(D_1B^2+\Sigma_1)}+\frac{1}{v_2(D_2B^2+\Sigma_2)}\right.\\ &\quad\left.\times\left(k_d-\frac{\nu\Sigma_{f,1}}{k_d(D_1B^2+\Sigma_1)}\right)\frac{D_2B^2+\Sigma_2}{\nu\Sigma_{f,2}}\right)\\ &=\frac{1}{k_d}\left(w_{1,2G\to 1G}\Lambda_1+w_{2,2G\to 1G}\Lambda_2\right).\end{aligned} \tag{34}$$

Assuming that the system is purely thermal, i.e. $\nu\Sigma_{f,1}=0$, the lifetime for the one-group model reduces to

$$\Lambda_{2G\to 1G}=\frac{1}{k_d}\left(\frac{1}{v_1(D_1B^2+\Sigma_1)}+\frac{1}{v_2(D_2B^2+\Sigma_2)}\frac{\Sigma_{1\to 2}}{D_1B^2+\Sigma_1}\right) \tag{35}$$

which is an extension of Eq. (3) to off-critical systems.

In the presence of an external source, the direct and adjoint models become

$$\begin{cases}(D_1B^2+\Sigma_1-\nu\Sigma_{f,1})\phi_1-\nu\Sigma_{f,2}\phi_2=S_1\\ -\Sigma_{1\to 2}\phi_1+(D_2B^2+\Sigma_2)\phi_2=0\end{cases} \tag{36}$$

and

$$\begin{cases}(D_1B^2+\Sigma_1-\nu\Sigma_{f,1})\phi_1^\dagger-\Sigma_{1\to 2}\phi_2^\dagger=\nu\Sigma_{f,1}\\ -\nu\Sigma_{f,2}\phi_1^\dagger+(D_2B^2+\Sigma_2)\phi_2^\dagger=\nu\Sigma_{f,2},\end{cases} \tag{37}$$

respectively. The solutions of the two algebraic systems are

$$\vec{\phi}=\begin{pmatrix}\dfrac{S_1}{(D_1B^2+\Sigma_1)(1-k_d)}\\ \dfrac{S_1\Sigma_{1\to 2}}{(D_1B^2+\Sigma_1)(D_2B^2+\Sigma_2)(1-k_d)}\end{pmatrix}, \tag{38}$$

and

$$\vec{\phi}^\dagger=\begin{pmatrix}\dfrac{k_d}{1-k_d}\\ \dfrac{1}{1-k_d}\dfrac{\nu\Sigma_{f,2}}{(D_2B^2+\Sigma_2)}.\end{pmatrix}. \tag{39}$$

Table 4
Nuclear data for a system characterized by thermal fissions only. The diffusion coefficient in two-group is calculated as $D_g = \frac{1}{3\Sigma_{t,g}}$.

	Two-group		One-group
	$g = 1$	$g = 2$	
$\Sigma_{t,g}$ [cm^{-1}]	0.354	0.409	0.3711
$\Sigma_{a,g}$ [cm^{-1}]	$9.78 \cdot 10^{-4}$	$5.56 \cdot 10^{-3}$	$2.404 \cdot 10^{-3}$
$\Sigma_{g\to g+1}$ [cm^{-1}]	$3.08 \cdot 10^{-3}$	–	–
$\nu\Sigma_{f,g}$ [cm^{-1}]	–	$1.22 \cdot 10^{-2}$	$3.795 \cdot 10^{-3}$
D_g [cm]	0.942	0.815	0.9022
v_g [cm/s]	$1.65 \cdot 10^{7}$	$5.5 \cdot 10^{5}$	$1.65 \cdot 10^{6}$

Table 5
Nuclear data for a system with non-zero fission cross sections in both groups. The diffusion coefficient in two-group is calculated as $D_g = \frac{1}{3\Sigma_{t,g}}$.

	Two-group		One-group
	$g = 1$	$g = 2$	
$\Sigma_{t,g}$ [cm^{-1}]	0.157	0.227	0.1632
$\Sigma_{a,g}$ [cm^{-1}]	$9.64 \cdot 10^{-5}$	$7.24 \cdot 10^{-4}$	$1.471 \cdot 10^{-4}$
$\Sigma_{g\to g+1}$ [cm^{-1}]	$2.63 \cdot 10^{-4}$	–	–
$\nu\Sigma_{f,g}$ [cm^{-1}]	$2.46 \cdot 10^{-3}$	$1.32 \cdot 10^{-2}$	$3.329 \cdot 10^{-3}$
D_g [cm]	2.123	1.468	2.064
v_g [cm/s]	$4.5 \cdot 10^{8}$	$1.0 \cdot 10^{7}$	$9.9 \cdot 10^{7}$

The effective lifetime computed using the source-driven shape turns out to be

$$\Lambda_{2G} = \frac{1}{k_d}\left(\frac{k_d}{v_1(D_1B^2+\Sigma_1)} + \frac{1}{v_2(D_2B^2+\Sigma_2)} \times \left(k_d - \frac{\nu\Sigma_{f,1}}{k_d(D_1B^2+\Sigma_1)}\right)\frac{\Sigma_{1\to2}}{D_1B^2+\Sigma_1}\right). \tag{40}$$

In case there is no fast fission, the effective lifetime is simply the sum of the fast and thermal lifetimes,

$$\Lambda_{2G} = \frac{1}{k_d}\left(\frac{1}{v_1(D_1B^2+\Sigma_1)} + \frac{1}{v_2(D_2B^2+\Sigma_2)}\right). \tag{41}$$

Eq. (41) has the same structure of Eq. (2), which was obtained for a critical system. Consequently, collapsing the model into a single group yields an expression similar to Eq. (3),

$$\begin{aligned}\Lambda_{2G\to1G} &= \frac{1}{k_d}\left(\frac{1}{v_1(D_1B^2+\Sigma_1)} + \frac{1}{v_2(D_2B^2+\Sigma_2)}\frac{\Sigma_{1\to2}}{D_1B^2+\Sigma_1}\right)\\ &= \frac{1}{k_d}\left(w_{1,1G}\frac{1}{v_1(D_1B^2+\Sigma_1)} + w_{2,1G}\frac{1}{v_2(D_2B^2+\Sigma_2)}\right).\end{aligned} \tag{42}$$

2.7. Results for the analytical cases

The formulae presented are now applied to test cases to provide quantitative evaluations of the effects identified. At first, a homogeneous spherical geometry is considered, with radius $R = 80$ cm, using the two-group material data reported in Table 4, where also the corresponding collapsed 1-group data are given. The calculation of the effective lifetimes provides the following results:

$$\begin{aligned}&\Lambda_{2G} = 2.8 \cdot 10^{-4}\ \text{s},\\ &\Lambda_{1G} = 1.6 \cdot 10^{-4}\ \text{s},\\ &\frac{|\Lambda_{1G} - \Lambda_{2G}|}{\Lambda_{2G}} = 42\%.\end{aligned} \tag{43}$$

The difference between the two values appears to be significant. In fact, differences of this magnitude may produce important effects on direct kinetic evaluations or inverse experimental interpretations, as Λ determines the time scale of response of the reactor.

Using the material data given in Table 5 the following values of the effective lifetimes are obtained:

$$\begin{aligned}&\Lambda_{2G} = 1.1 \cdot 10^{-5}\ \text{s},\\ &\Lambda_{1G} = 3.0 \cdot 10^{-6}\ \text{s},\\ &\frac{|\Lambda_{1G} - \Lambda_{2G}|}{\Lambda_{2G}} = 73\%,\end{aligned} \tag{44}$$

which again highlight a significant difference.

Results produced without adjoint weighting, using the same data as in the previous two cases, show that the collapsing to one-group is not affecting the lifetime value, as the process consistently preserves the reaction rates:

- thermal system

$$\Lambda_{2G,\text{no weight}} = 1.6 \cdot 10^{-4}\ \text{s}; \tag{45}$$

- fast system

$$\Lambda_{2G,\text{no weight}} = 3.0 \cdot 10^{-6}\ \text{s}. \tag{46}$$

For the thermal case, the equivalence of this 2-group formulation with the 1-group definition is evident, while in the case of a fast system the equivalence appears clearly, once the proper criticality condition is applied.

3. Results for some numerical cases

For a second set of results, four homogeneous cylinders featured by the typical spectrum of a LWR, MSFR, SFR and LFR are considered. The reference values of k_{eff} and Λ are initially computed with a set of 8-group constants, generated with the Serpent code. Each system is made critical by properly adjusting ν, with the aim of testing different collapsing strategies towards a lower number of groups and comparing the Λ values and the criticality level. The original energy structure is given in Table 6, as well as the energy boundaries adopted for the progressive collapsing towards one group.

In the following, the group lifetimes are computed using two definitions for the group-wise velocities. The first one, indicated as $\bar{v}_{g,KE}$, is computed from the definition of kinetic energy arithmetic average (KE) in the group, following the approach used in the ERANOS code (Rimpault et al., 2002),

$$\begin{aligned}\bar{v}_{g,KE} &= \sqrt{\frac{2}{m_n}\frac{E_g + E_{g+1}}{2}} = C_{\text{m}\to\text{cm}}\sqrt{2\frac{C_{\text{MeV}\to\text{J}}}{m_n}}\sqrt{\frac{v_g + v_{g+1}}{2}}\\ &\approx 9.86\sqrt{v_g + v_{g+1}},\end{aligned} \tag{47}$$

where $C_{\text{m}\to\text{cm}} = 100\,\frac{\text{cm}}{\text{m}}$, $m_n = 1.6749 \cdot 10^{-27}$ kg is the neutron mass, $C_{\text{MeV}\to\text{J}} = 1.6022 \cdot 10^{-13}\,\frac{\text{J}}{\text{MeV}}$ and v_g and v_{g+1} are the velocities at the lower and upper group boundaries. The other set of group-averaged velocities, indicated with $\bar{v}_{g,ND}$, is computed by preserving the neutron density (ND) in each group,

$$\frac{1}{\bar{v}_{g,ND}} = \frac{\int_{E_g}^{E_{g+1}} dE\,\frac{1}{v(E)}\phi(E)}{\int_{E_g}^{E_{g+1}} dE\,\phi(E)} = \frac{\int_{E_g}^{E_{g+1}} dE\,n(E)}{\int_{E_g}^{E_{g+1}} dE\,\phi(E)}. \tag{48}$$

The adoption of these different average velocities has an important impact on the values of the group-wise lifetimes, as it can be seen in the following.

Tables 7 through 10 report Λ and k_{eff} for the four configurations analysed previously. The effective lifetime is computed either by using a group-averaged $1/v_g$ that preserves the neutron density (indicated with Λ_{ND} in the tables) or by using $1/v_g$ defined according to the approach used in ERANOS, which preserves the average kinetic energy (indicated with Λ_{KE} in the tables). In all three cases, the adoption of the inverse group velocity computed with Eq. (47) yields very poor estimates of the effective lifetime, suggesting that using an effective inverse velocity that preserves the neutron density is more physically consistent. Concerning this last approach, Λ is always underestimated

Table 6
Group structures adopted for the calculation of k_{eff} and Λ in the cases of LWR, LFR and MSFR systems.

8	$2 \cdot 10^{1}$	$1 \cdot 10^{0}$	$1 \cdot 10^{-1}$	$1 \cdot 10^{-2}$	$1 \cdot 10^{-3}$	$1 \cdot 10^{-4}$	$1 \cdot 10^{-5}$	$6.25 \cdot 10^{-7}$	$1 \cdot 10^{-11}$
7	x	x		x	x	x	x	x	x
6	x	x		x	x	x		x	x
5	x	x		x		x		x	x
4	x	x		x				x	x
3	x			x				x	x
2	x							x	x
1	x								x

Table 7
k_{eff} and Λ evaluated with the energy structures reported in Table 6 for a thermal (LWR-like) system.

Number of groups	Λ_{ND} [μs]	% $\frac{\Lambda_{8g}-\Lambda_i}{\Lambda_{8g}}$	Λ_{KE} [μs]	% $\frac{\Lambda_{8g}-\Lambda_i}{\Lambda_{8g}}$	k_{eff}	$\lvert k_{\text{eff,8g}} - k_{\text{eff,i}} \rvert$ [pcm]
8	21.474	–	21.474	–	1.000000	–
7	21.452	+0.10	11.742	+45.32	1.001120	+111.99
6	21.333	+0.65	10.996	+48.79	1.001122	+112.24
5	21.331	+0.67	10.927	+49.11	1.001123	+112.28
4	21.179	+1.37	10.837	+49.53	1.008232	+823.23
3	21.072	+1.87	10.214	+52.44	1.008236	+823.56
2	20.903	+2.66	10.063	+53.14	1.014556	+1455.64
1	16.934	+21.14	0.010	+99.95	1.019077	+1907.70

Table 8
k_{eff} and Λ evaluated with the energy structures reported in Table 6 for a fast (SFR-like) system.

Number of groups	Λ_{ND} [μs]	% $\frac{\Lambda_{8g}-\Lambda_i}{\Lambda_{8g}}$	Λ_{KE} [μs]	% $\frac{\Lambda_{8g}-\Lambda_i}{\Lambda_{8g}}$	k_{eff}	$\lvert k_{\text{eff,8g}} - k_{\text{eff,i}} \rvert$ [pcm]
8	0.398	–	0.398	–	1.000000	–
7	0.435	+9.17	0.265	+33.45	1.010422	+1042.21
6	0.467	+17.22	0.259	+34.88	1.010422	+1042.21
5	0.473	+18.74	0.235	+40.95	1.010525	+1052.49
4	0.510	+28.00	0.159	+60.15	1.017647	+1764.67
3	0.584	+46.64	0.136	+65.76	1.004322	+432.21
2	0.872	+119.00	0.045	+88.71	1.038419	+3841.89
1	0.884	+121.98	0.034	+91.46	1.038460	+3845.96

Table 9
k_{eff} and Λ evaluated with the energy structures reported in Table 6 for a fast (LFR-like) system.

Number of groups	Λ_{ND} [μs]	% $\frac{\Lambda_{8g}-\Lambda_i}{\Lambda_{8g}}$	Λ_{KE} [μs]	% $\frac{\Lambda_{8g}-\Lambda_i}{\Lambda_{8g}}$	k_{eff}	$\lvert k_{\text{eff,8g}} - k_{\text{eff,i}} \rvert$ [pcm]
8	0.442	–	0.442	–	1.000000	–
7	0.466	+5.34	0.275	+37.71	1.006104	+610.38
6	0.471	+6.63	0.274	+37.96	1.006104	+610.38
5	0.467	+5.70	0.249	+43.65	1.006106	+610.63
4	0.504	+13.98	0.157	+64.40	1.011387	+1138.72
3	0.485	+9.71	0.142	+58.00	1.011388	+1138.79
2	0.600	+35.67	0.040	+91.00	1.016334	+1633.35
1	0.601	+35.89	0.039	+91.24	1.016334	+1633.39

in the LWR case, while in the LFR and SFR cases it is always overestimated. This confirms the observations drawn previously in the paper. Since the effective lifetime describes the time scale between neutron generations in a multiplying system, its overestimation is an undesired effect, especially for fast systems, whose dynamics is notoriously more challenging (see Tables 8 and 9).

The MSFR shows an intermediate behaviour, overestimating Λ when more than 3 groups are used and underestimating it when 3 groups or less are employed.

Fig. 1, which shows the group-wise direct and adjoint fluxes for the three systems in the 8- and 3-group cases, helps to understand this behaviour. The MSFR spectrum in the 8-group case is quite similar to the one of the LFR, but with a larger fraction of thermal neutrons, while in the 3-group case the MSFR flux approaches the LWR spectrum in the epithermal group. A similar behaviour occurs also for the adjoint spectrum, suggesting that, when the energy model adopted is simple, the MSFR behaves more like a thermal system than a fast system, while, when the energy group model is more accurate, the MSFR presents the usual characteristics of a fast system. These observations are further supported by the analytical results already discussed in Section 2.3 and Section 2.4.

Concerning the magnitude of the relative differences with respect to the reference 8-group case in Table 7 through 10, the LWR seems the system that is affected the less by the energy model, when more than 1 group is adopted, while the SFR and LFR are the most sensitive to the energy discretization. Also in this case, the MSFR shows intermediate features. The low sensitivity of the LWR-like system may be explained by the small contribution of the fast groups to the total importance $\langle \phi^{\dagger} | \hat{\mathbb{V}}^{-1} \phi \rangle$: the terms $1/\bar{v}_g$ are much smaller than $1/v_8$, and the adjoint fluxes in the fast groups are generally lower than the thermal ones. Conversely, in the fast systems, both the direct and adjoint fast fluxes are quite large, justifying the significant error obtained when the fast

Table 10
k_{eff} and Λ evaluated with the energy structures reported in Table 6 for a fast (MSFR-like) system.

Number of groups	Λ_{ND} [μs]	% $\frac{\Lambda_{8g}-\Lambda_i}{\Lambda_{8g}}$	Λ_{KE} [μs]	% $\frac{\Lambda_{8g}-\Lambda_i}{\Lambda_{8g}}$	k_{eff}	$\lvert k_{\text{eff,8g}}-k_{\text{eff,i}}\rvert$ [pcm]
8	1.019	–	0.819	–	1.000000	–
7	1.021	+0.17	0.719	+29.47	1.000232	+23.25
6	1.094	+7.34	0.729	+28.43	1.000244	+24.42
5	1.053	+3.36	0.575	+43.57	1.000622	+62.18
4	1.053	+3.33	0.511	+49.86	1.003586	+358.56
3	0.943	−7.49	0.287	+71.81	1.003973	+397.31
2	0.960	−5.74	0.040	+96.10	1.004002	+400.25
1	0.970	−4.78	0.029	+97.12	1.004041	+401.43

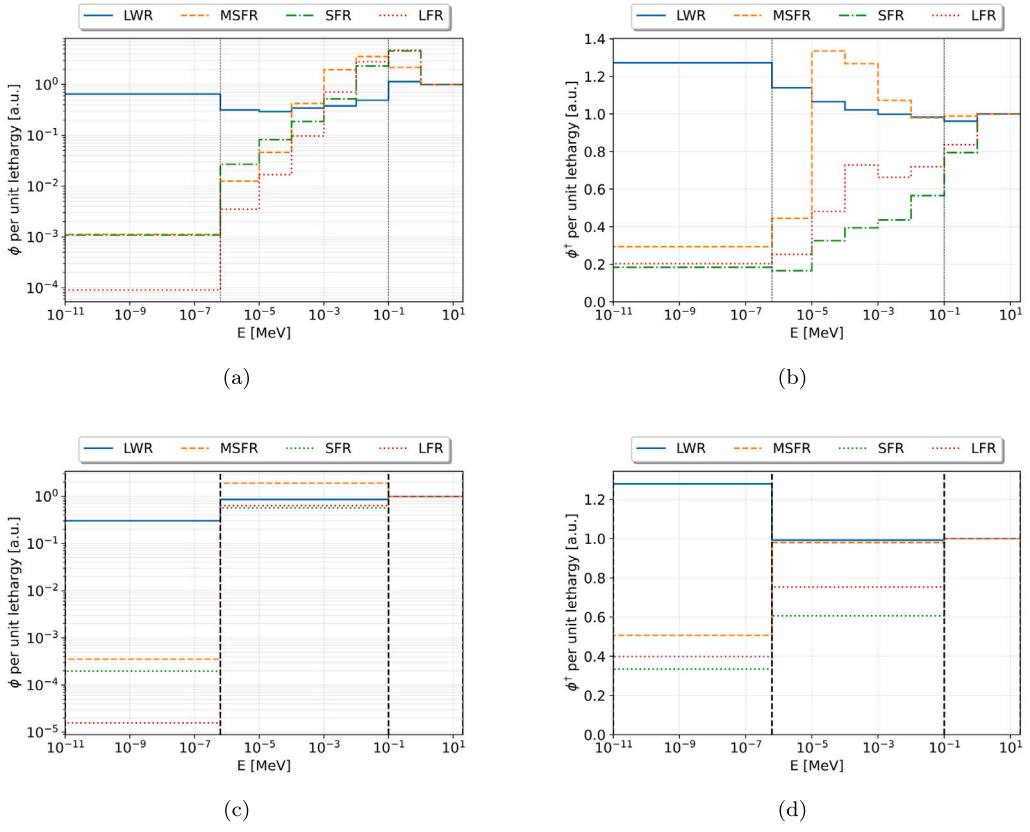

Fig. 1. Direct (left) and adjoint (right) spectra for the LWR-, MSFR- and LFR-like systems computed on the 8-group (top) and 3-group (bottom) structures. The vertical dashed lines represent the group boundaries used in the 3-group structures.

groups are collapsed. This observation suggests to explore the effects of alternative collapsing techniques that take into account also the role of the adjoint in the definition of the effective lifetime. Hence, the following set of results concerns the comparison of results obtained when the nuclear data collapsing is performed preserving the reaction rates (lower index RR) and the adjoint-weighted reaction rates (AWRR). In this last case, the velocity is collapsed preserving the total importance $\langle\phi^{\dagger}|\hat{\mathbb{V}}^{-1}\phi\rangle$. The LWR, SFR, LFR and MSFR configurations are provided in Tables 11 through 14, where the first column coincides with the results of Tables 11, Table 12, Table 13 and Table 14, where the first column coincides with the results of Tables 7 through 10 and is reported to facilitate the comparison. The collapsing based on preserving adjoint-weighted reaction rates is consistent with the weighted integral in the Λ definition, thus the energy collapsing has an almost negligible effect on the Λ value for all the systems analysed, provided that more than 3–4 groups are employed. The only remaining discrepancies is to be attributed to the diffusion coefficient value.

Table 11
Λ evaluated with the energy structures reported in Table 6 for a fast (LWR-like) system adopting different collapsing approaches for the group constants. The reference Λ computed with 8 groups is 21.474 ms.

Number of groups	Λ_{RR} [μs]	% $\frac{\Lambda_{8g}-\Lambda_i}{\Lambda_{8g}}$	Λ_{AWRR} [μs]	% $\frac{\Lambda_{8g}-\Lambda_i}{\Lambda_{8g}}$
7	21.452	+0.10	21.448	+0.12
6	21.333	+0.65	21.348	+0.58
5	21.331	+0.67	21.341	+0.62
4	21.179	+1.37	21.141	+1.55
3	21.072	+1.87	20.952	+2.43
2	20.903	+2.66	21.093	+1.77
1	16.934	+21.1	17.449	+18.74

An additional set of results concerns the experimental facility KUCA (Pyeon et al., 2007), again comparing different ways to generate few-group energy structures starting from an eight-group constants database. The energy configurations adopted are given in Table 15, and

Table 12
Λ evaluated with the energy structures reported in Table 6 for a fast (LFR-like) system adopting different collapsing approaches for the group constants. The reference Λ computed with 8 groups is 0.442 ms.

Number of groups	Λ_{RR} [μs]	% $\frac{\Lambda_{8g}-\Lambda_i}{\Lambda_{8g}}$	Λ_{AWRR} [μs]	% $\frac{\Lambda_{8g}-\Lambda_i}{\Lambda_{8g}}$
7	0.466	+5.34	0.444	+0.55
6	0.471	+6.63	0.449	+1.49
5	0.467	+5.70	0.448	+1.47
4	0.504	+13.98	0.449	+1.62
3	0.485	+9.71	0.439	+0.60
2	0.600	+35.67	0.504	+14.13
1	0.601	+35.89	0.505	+14.17

Table 13
Λ evaluated with the energy structures reported in Table 6 for a fast (SFR-like) system adopting different collapsing approaches for the group constants. The reference Λ computed with 8 groups is 0.398 ms.

Number of groups	Λ_{RR} [μs]	% $\frac{\Lambda_{8g}-\Lambda_i}{\Lambda_{8g}}$	Λ_{AWRR} [μs]	% $\frac{\Lambda_{8g}-\Lambda_i}{\Lambda_{8g}}$
7	0.435	+9.17	0.377	+5.25
6	0.467	+17.22	0.407	+2.29
5	0.473	+18.74	0.404	+1.41
4	0.510	+28.00	0.384	+3.54
3	0.584	+46.64	0.416	+4.44
2	0.872	+119.00	0.468	+17.60
1	0.884	+121.98	0.471	+18.36

Table 14
Λ evaluated with the energy structures reported in Table 6 for a fast (MSFR-like) system adopting different collapsing approaches for the group constants. The reference Λ computed with 8 groups is 1.019 ms.

Number of groups	Λ_{RR} [μs]	% $\frac{\Lambda_{8g}-\Lambda_i}{\Lambda_{8g}}$	Λ_{AWRR} [μs]	% $\frac{\Lambda_{8g}-\Lambda_i}{\Lambda_{8g}}$
7	1.021	+0.17	1.020	+0.07
6	1.094	+7.34	1.046	+2.70
5	1.053	+3.36	1.027	+0.84
4	1.053	+3.33	1.025	+0.63
3	0.943	−7.49	0.925	−9.25
2	0.960	−5.74	0.951	−6.67
1	0.970	−4.78	0.952	−6.55

the corresponding results for Λ and k_{eff} are in Table 16. As done for the previous cases, results are provided with two different definitions of $1/v_g$, confirming both the effect of the collapsing to a small number of groups and the impact of the velocity definition.

4. Collapsing for a very fine group structure

To verify the conclusions that can be drawn from the elementary cases analysed in the previous section, we now take into consideration a more realistic situation where at the beginning the full complexity of energy dependence is retained: to this aim, an energy collapsing procedure that starts from a large number of energy groups has been carried out.

4.1. Homogeneous spherical system

At first, a homogeneous system with a mixture of $25wt\%U-235/U$ enriched uranium and lead is assumed, in space asymptotic configuration with different values of the geometrical buckling: this choice allows to still treat the problem analytically. Different values of the geometrical buckling are used to simulate systems of different physical dimensions and the atomic density of uranium is adjusted in order to have a critical system in all the configurations. The reference energy structure is based on 1000 groups and a constant spectrum is assumed within each group to obtain averaged cross-sections, as this approximation is quite accurate for such a large number of groups. The resulting neutron spectra is reported in Fig. 2, where R represents the geometrical dimension in spherical geometry. The spectrum evaluation is carried out analytically. As it can be seen from the graphs, the spectrum is hardening as the system gets smaller, due to increased leakage, while for a larger system the effect of scattering is not negligible and eventually leads to thermalization.

Table 15
Group structures adopted for the calculation of k_{eff} and Λ for the KUCA system.

4	1.9640 $\cdot 10^1$	1.0024 $\cdot 10^0$	1.0078 $\cdot 10^{-2}$	1.02$\cdot 10^{-6}$	1 $\cdot 10^{-11}$
3A	x		x	x	x
3B	x	x	x	x	
3C	x	x	x		x
2A	x			x	x
2B	x	x			x
2C	x		x		x

The effective lifetime is calculated in the reference configuration and compared to the results obtained when collapsing to a reduced number of energy groups (of constant width in lethargy): in Fig. 3 the lifetime value as a function of the number of energy groups is reported: for this material composition the reduction of the number of groups leads to an increase of the value of Λ, in analogy to the LFR case discussed before.

Furthermore, it can be observed that in this case the change in lifetime due to the collapsing procedure is more relevant (up to 20%) for softer-spectrum systems, while being much less relevant for hard-spectrum systems. The graphs show that the effect is relevant only when collapsing to a "small" number of groups, thus providing a guideline for the minimum number of groups to be used in order to obtain an estimate of Λ which is not too much dependent on the energy structure. From the graphs it appears that such a critical number of groups is around 100.

4.2. Application to a heterogeneous configuration

The next step of the analysis is focused on a more realistic, heterogeneous configuration in both critical and subcritical mode. A cylindrical $r-z$ geometry of a core constituted by a mixture of 18% U ($30wt\%U-235/U$ enriched) and of 82% Lead, surrounded by a lead reflector, is considered (see Fig. 4 for both critical and subcritical configurations). Calculations are performed with the ERANOS code (Rimpault et al., 2002) assuming different energy structures.

The resulting lifetimes values are reported in Tables 17 and 18. These results are consistent with the previous evaluations and they show that most of the effect appears when collapsing to a small number of groups, namely below 49.

5. Conclusions

A study of the effect of the group energy structure on the estimated values of the effective neutron lifetime is carried out. The analysis has been performed at first in a simple space asymptotic approach, allowing for a full analytical solution and for an interpretation of the physical dependence of Λ on the energy grid. The results show that the energy collapsing procedure is impacting on the effective lifetime evaluation mostly when a small numbers of groups are employed. The analysis shows that the effect may significantly vary both in absolute value and in sign, depending on the physical characteristics of the system considered (energy spectrum, number of groups and group structure). In fact, when comparing the case of thermal and fast systems, the change of Λ may result in non-conservative evaluations of the time-dependent behaviour of a nuclear reactor core. This phenomenon is especially serious for fast reactors, as it may lead to non-conservative results.

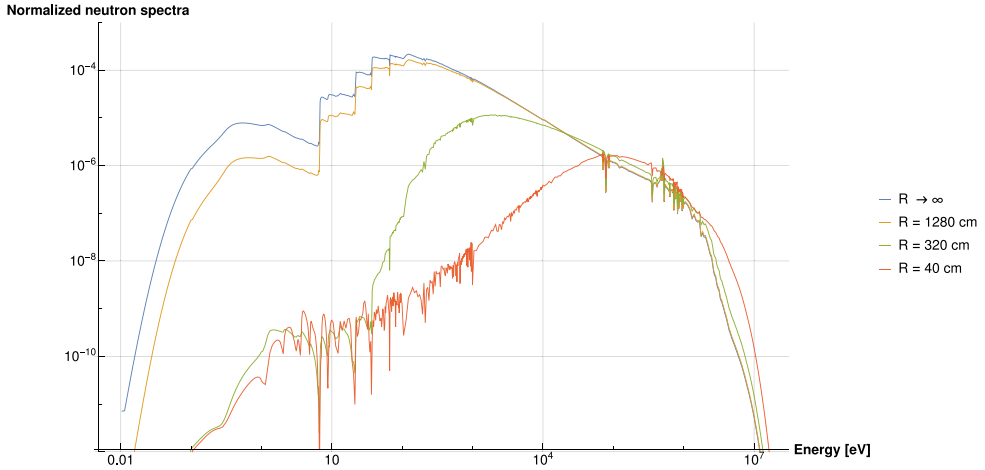

Fig. 2. Energy spectra for homogeneous system with different dimension R. 1000 energy groups considered.

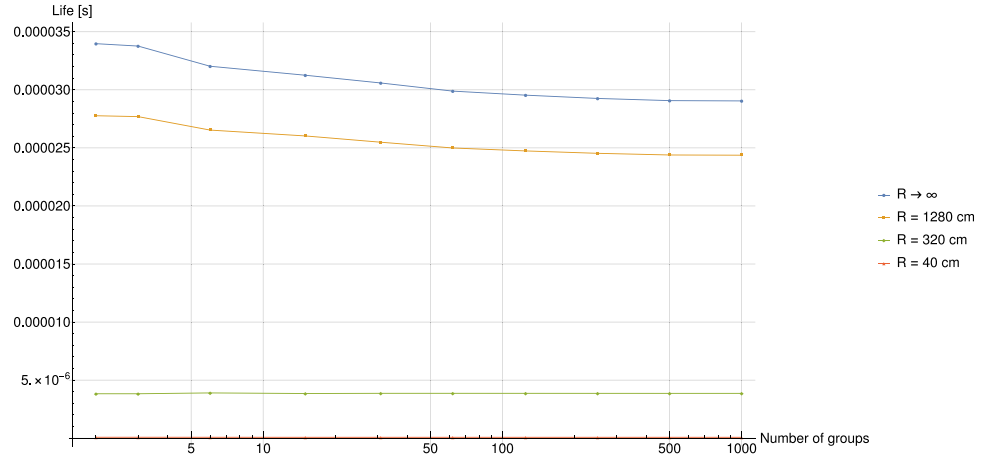

Fig. 3. Effective lifetime for the homogeneous medium as a function of the energy group structure.

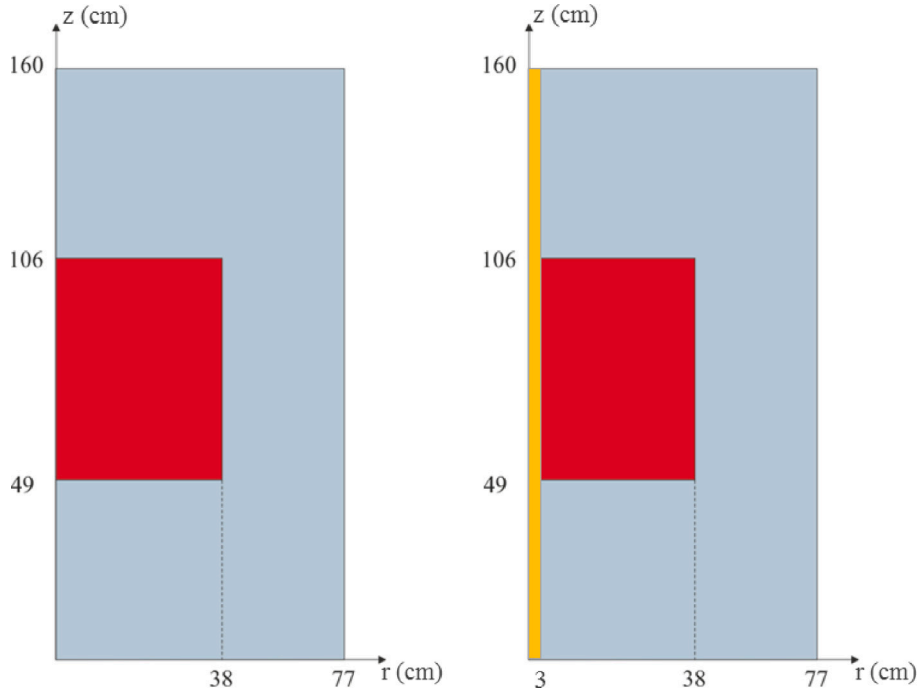

Fig. 4. Geometrical domain adopted for ERANOS simulations. Left: critical configuration; Right: subcritical configuration. Red — core; grey — reflector; orange — source channel.

Table 16
k_{eff} and Λ evaluated with the energy structures reported in Table 15 and by collapsing the neutron speed preserving the neutron density.

Group structure	Λ [μs]	% rel. err.	Λ_{KE} [μs]	% rel. err.	k_{eff}	abs. err. [pcm]
4	4.238	–	4.2376	–	1.00000	–
3A	4.209	0.67	4.1991	0.91	1.00670	670
3B	4.228	0.22	4.1186	2.81	1.00127	127
3C	3.909	7.76	0.1771	95.82	1.00670	49
2A	4.180	1.37	4.0534	4.35	1.00670	1177
2B	3.853	9.07	0.0316	99.25	1.00272	272
2C	3.883	8.37	0.1656	96.09	1.00719	719
1	3.761	11.25	0.0087	99.89	1.01484	1484

Table 17
k_{eff} and Λ evaluated with the ERANOS code for a critical fast system assuming different energy structures.

N. of groups	Λ [μs]	$\% \frac{\Lambda_{8g} - \Lambda_i}{\Lambda_{8g}}$
295	0.702	
172	0.694	1.140
49	0.654	6.838
15	0.591	15.812
4	0.313	55.413

Table 18
k_{eff} and Λ evaluated with the ERANOS code for a subcritical fast system (k_{eff} around 0.98) assuming different energy structures.

N. of groups	Λ [μs]	$\% \frac{\Lambda_{8g} - \Lambda_i}{\Lambda_{8g}}$
295	0.704	
172	0.698	0.852
49	0.659	6.392
15	0.597	15.199
4	0.315	55.256

Declaration of competing interest

The authors declare that they have no known competing financial interests or personal relationships that could have appeared to influence the work reported in this paper.

Acknowledgements

This work is supported in part by a grant from Compagnia di San Paolo - Torino (Italy) through the project "OCAPIE" (grant #9535). This work has been carried out under the auspices of the Italian National Group of Mathematical Physics (Gruppo Nazionale di Fisica Matematica, GNFM) of the National Institute of High Mathematics (Instituto Nazionale di Alta Matematica, INDAM)

Data availability

The complete datasets and scripts employed to execute and post-process the calculations presented in this paper are available in https://doi.org/10.5281/zenodo.14454835 open access repository on Zenodo.

References

Abrate, N., Aimetta, A., Dulla, S., Pedroni, N., 2023a. Nuclear data uncertainty propagation for the molten salt fast reactor design. Nucl. Sci. Eng. 197 (12), 2977–2999, URL https://doi.org/10.1080/00295639.2023.2190861.

Abrate, N., Aufiero, M., Dulla, S., Fiorito, L., 2019. Nuclear data uncertainty quantification in molten salt reactors with XGPT. In: Proceedings of the ANS International Conference M&C2019, Portland, OR.

Abrate, N., Burrone, M., Dulla, S., Ravetto, P., Saracco, P., 2020. Eigenvalue formulations for the P_N approximation to the neutron transport equation. J. Comput. Theor. Transp. 50 (5), http://dx.doi.org/10.1080/23324309.2020.1856879.

Abrate, N., Dulla, S., Pedroni, N., 2023b. A non-intrusive reduced order model for the characterisation of the spatial power distribution in large thermal reactors. Ann. Nucl. Energy 184, 109674, URL https://doi.org/10.1016/j.anucene.2022.109674.

Abrate, N., Dulla, S., Ravetto, P., Saracco, P., 2021. On some features of the eigenvalue problem for the P_N approximation of the neutron transport equation. Ann. Nucl. Energy 163, 108–477, URL https://www.sciencedirect.com/science/article/pii/S0306454921003534.

Bell, G.I., Glasstone, S., 1970. Nuclear Reactor Theory. New, Van Nostrand Reinhold Company, New York.

Duderstadt, J.J., Hamilton, L.J., 1976. Nuclear Reactor Analysis. Wiley, New York.

Dulla, S., Cadinu, F., Picca, P., Ravetto, P., 2006. Effects of neutron source characteristics in direct and adjoint problems for subcritical systems. Int. J. Nucl. Energy Sci. Technol. 2 (4), 361–377.

Dulla, S., Nervo, M., Ravetto, P., Saracco, P., Lomonaco, G., Carta, M., 2015. Reflector effects on the kinetic response in subcritical systems. In: Proceedings of the Joint International Conference on Mathematics and Computation, Supercomputing in Nuclear Applications and the Monte Carlo Method (ANS M&C+ SNA+ MC 2015), Nashville, USA.

Dulla, S., Ravetto, P., Saracco, P., Borreani, W., Carta, M., Fabrizio, V., Peluso, V., 2018. Energy models for the evaluation of the effective neutron lifetime. In: Proceedings of International Conference on the Physics of Nuclear Reactors PHYSOR2018, Cancun, Mexico.

Fei, T., Mohamed, A., 2013. Neutronics Benchmark Specifications for EBR-II Shutdown Heat Removal Test SHRT-45R-Revision 1. Technical report, Argonne National Lab.(ANL), Argonne, IL (United States).

Grasso, G., Petrovich, C., Mattioli, D., Artioli, C., Sciora, P., Gugiu, D., Bandini, G., Bubelis, E., Mikityuk, K., 2014. The core design of ALFRED, a demonstrator for the European lead-cooled reactors. Nucl. Eng. Des. 278, 287–301, URL https://www.sciencedirect.com/science/article/pii/S0029549314004361.

Henry, A.F., 1958. The application of reactor kinetics to the analysis of experiments. Nucl. Sci. Eng. 3 (1), 52–70.

Ivanov, K., Avramova, M., Kamerow, S., Kodeli, I.A., Sartori, E., Ivanov, E., Cabellos, O., 2013. Benchmark for Uncertainty Analysis in Modeling (UAM) for Design, Operation and Safety Analysis of LWRs, vol. 1, OECD Nuclear Energy Agency.

Kiefhaber, E., 1969. Comment on the calculation of neutron lifetime. Nucl. Sci. Eng. 38 (2), 178–179.

Leppänen, J., Pusa, M., Viitanen, T., Valtavirta, V., Kaltiaisenaho, T., 2015. The serpent Monte Carlo code: Status, development and applications in 2013. Ann. Nucl. Energy (ISSN: 18732100) 82, 142–150. http://dx.doi.org/10.1016/j.anucene.2014.08.024.

Pyeon, C.H., Hirano, Y., Misawa, T., Unesaki, H., Ichihara, C., Iwasaki, T., Shiroya, S., 2007. Preliminary experiments on accelerator-driven subcritical reactor with pulsed neutron generator in Kyoto University Critical Assembly. J. Nucl. Sci. Technol. 44 (11), 1368–1378.

Rimpault, G., Plisson, D., Tommasi, J., Jacqmin, R., Rieunier, J., 2002. The ERANOS code and data system for fast reactor neutronic analyses. In: International Conference on Physics of Reactors, PHYSOR 2002, Seoul, South Korea. pp. 1134–1143.

Saracco, P., Dulla, S., Ravetto, P., 2012. On the spectrum of the multigroup diffusion equations. Prog. Nucl. Energy 59, 86–95.

Valocchi, G., Tommasi, J., 2024. Impact of the Multigroup Velocity Approximation in the Evaluation of the Effective Neutron Lifetime. In: International Conference on Physics of Reactors, PHYSOR 2024, San Francisco, CA.

Williams, M.L., 1991. Generalized contributon response theory. Nucl. Sci. Eng. 108 (4), 355–383.